EXPERIMENT 1: UNIFORM ACCELERATION

SAMUEL ELLISON – UID # 204977052

LAB PERFORMED ON 4/18/2018

LAB SECTION: WEDNESDAY 2PM

TA NAME: ERIK KRAMER

LAB PARTNERS: ERIC WONG AND MIKE MORIN

WORKSHEET

1 COVER SHEET (see above)

2 PLOTS

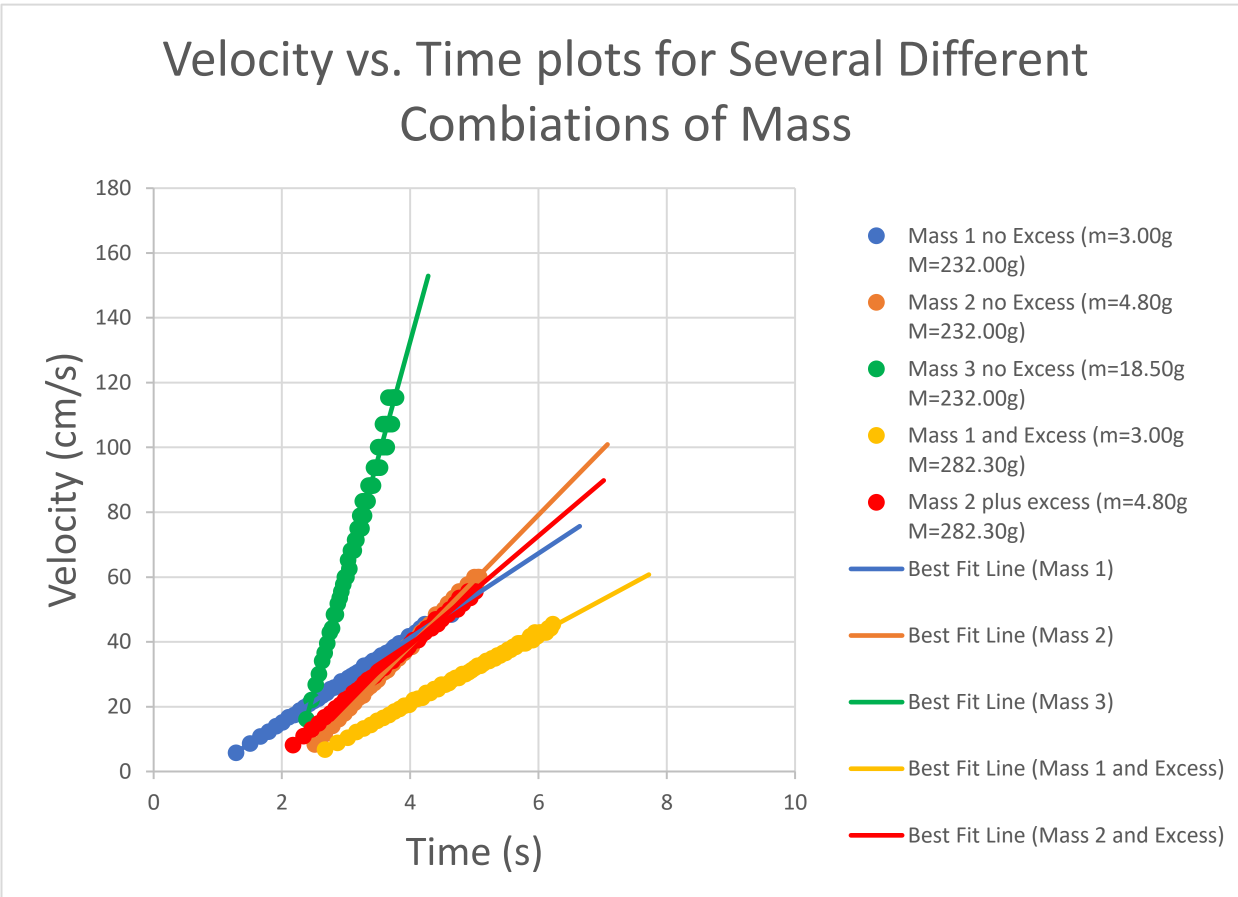

Figure 1: Five velocity vs. time plots. Each color represents a different set of masses m and M, the hanging mass and glider mass respectively. The slope of the best fit line is the average acceleration, see below:

Mass 1 no excess:	*Slope =*	*13.03 ± 0.06 cm/s²*
Mass 2 no Excess:	*Slope =*	*20.2 ± 0.1 cm/s²*
Mass 3 no Excess:	*Slope =*	*72.0 ± 0.8 cm/s²*
Mass 1 plus Excess:	*Slope =*	*10.67 ± 0.05 cm/s²*
Mass 2 plus Excess:	*Slope =*	*16.83 ± 0.09 cm/s²*

3 DATA TABLE

Trial	Hanging Mass m_{best} (g)	Glider Mass M_{best} (g)	Fit Acceleration a_{fit} (cm/s^2)	Predicted Acceleration $a_{predicted}$ (cm/s^2)
1	3.00	232.00	13.03 ± 0.06	12.5 ± 0.2
2	4.80	232.00	20.2 ± 0.1	19.9 ± 0.2
3	18.50	232.00	72.0 ± 0.8	72.4 ± 0.2
4	3.00	282.30	10.67 ± 0.05	10.3 ± 0.2
5	4.80	282.30	16.83 ± 0.09	16.4 ± 0.2

4 DERIVATIONS

Equation 1.1:

This equation is derived from Newton's second law:

$$\boldsymbol{F}_{net} = m\boldsymbol{a}$$

Where m is the mass of the body and a is its acceleration. We can divide the two masses, m and M (hanging mass and glider mass) into two systems and apply Newton's second law individually. We can assume that the accelerations of each of these bodies are equal since they are moving as a single system.

For the hanging mass, we have a weight force pulling it down in the positive direction, and a Tension force exerted by the string pulling it up in the negative direction. The net force acting on mass m is shown below:

$$\boldsymbol{F}_{net\text{-x},m} = \boldsymbol{W} - \boldsymbol{T}$$

OR

$$|F_{net\text{-x},m}| = mg - |T| = ma$$

For the glider, the only force acting it in its accelerating direction is the Tension force from the string, T, which we assume has the same magnitude as the Tension acting on the hanging mass. Therefore:

$$\boldsymbol{F}_{net\text{-x},M} = \boldsymbol{T}$$

OR

$$\left|F_{net\text{-x},M}\right| = |T| = Ma$$

Since we have two equations both with the Tension Force, we can simply substitute the second equation into the first, giving:

$$mg - Ma = ma$$

Solving for a:

$$a = \frac{gm}{m + M}$$

We have recovered equation 1.1.[1]

Uncertainties:

Let us define a_{fit} as the acceleration derived from the slope of the velocity vs. time plots, and $a_{\text{predicted}}$ to be the acceleration calculated from equation 1.1.

To derive the uncertainty for $a_{\text{predicted}}$ we can simplify equation 1.1 to be:

$$a = \frac{x}{y} \text{ where } x = gm \text{ and } y = m + M$$

Applying equation ii.23[1] in the manual, we have:

$$\delta a = |a_{\text{best}}| \sqrt{\left(\frac{\delta x}{|x_{\text{best}}|}\right)^2 + \left(\frac{\delta y}{|y_{\text{best}}|}\right)^2}$$

$$\text{Where: } a_{\text{best}} = \frac{x_{\text{best}}}{y_{\text{best}}},\ x_{\text{best}} = gm_{\text{best}},\ y_{\text{best}} = m_{\text{best}} + M_{\text{best}}$$

Applying Equation ii.21:[1]

$$\delta x = |g|\delta m$$

Applying Equation ii.22:[1]

$$\delta y = \sqrt{(\delta m)^2 + (\delta M)^2}$$

Substituting everything gives:

$$\delta a_{\text{predicted}} = \left|\frac{gm_{\text{best}}}{m_{\text{best}} + M_{\text{best}}}\right| \sqrt{\left(\frac{\delta m}{|m_{\text{best}}|}\right)^2 + \left(\frac{\sqrt{(\delta m)^2 + (\delta M)^2}}{|m_{\text{best}} + M_{\text{best}}|}\right)^2}$$

Calculations of $\delta a_{\text{predicted}}$ use the values for δm and δM as ±0.05g, as given from the balance.

The uncertainty for a_{fit} comes from the linear regression data analysis on excel.

5 CONCLUSION

The acceleration of a glider across a track can be determined several ways: experimentally or analytically. The application of Newton's second law provides the analytical acceleration while analysis of experimental measurements provides the experimental acceleration. A comparison between the fit acceleration from the plots created from experimental data and the predicted acceleration from equation 1.1 shows a strong similarity. We see the greatest difference between these values in trials 4 and 5, when a mass was added to the glider. This may infer that a possible explanation for the difference in these accelerations can be attributed to the glider's movement across the track. Although the track was prepared to be level, it is impossible to create a perfectly level track. Plus, there can't exist a "zero" friction track, there may be some resistance. In addition, when releasing the glider, there may have been a slight disturbance in the glider's initial motion. All of these can contribute to an error in the fit acceleration values. However, overall, we do observe a strong and expected connection between fit and predicted acceleration. The most effective way to improve this experiment would be to decrease any friction between the glider and track and to calibrate an extremely level surface and track to run the experiment on.

6 EXTRA CREDIT

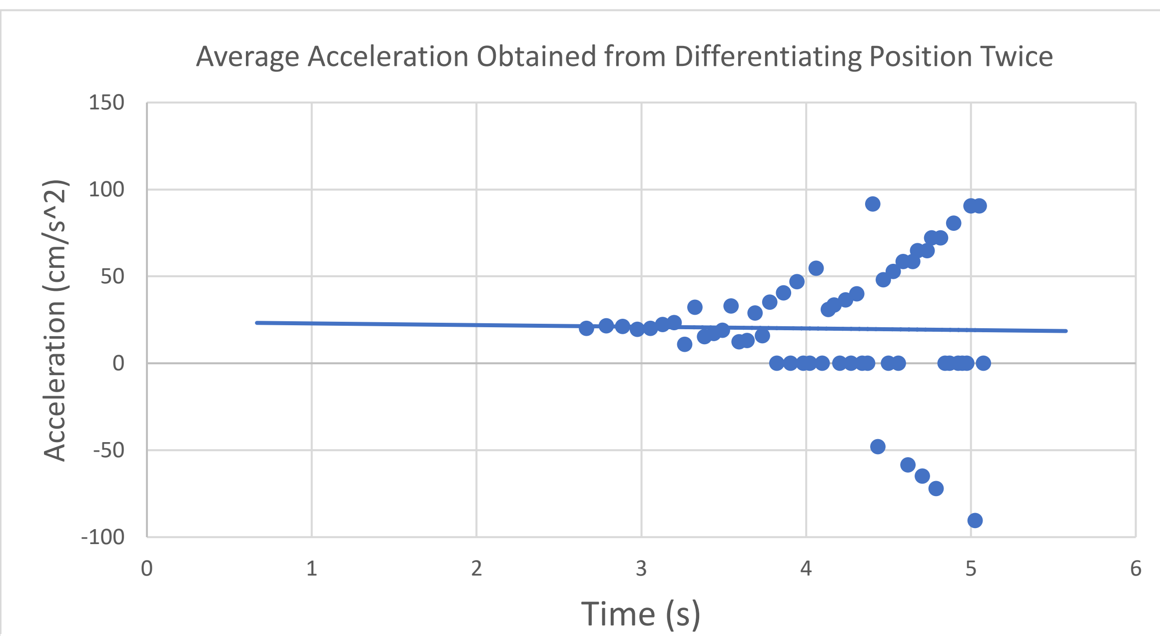

Figure 2: Acceleration vs. Time Plot for Trial 2 (m = 4.80g and M = 232.00g). Observe the increase in noise accompanying an increase in time. A line of best fit is provided to show approximate acceleration.

The plot above shows a set of data representing the second derivative of position x(t) as a function of time, which is a(t). In other words:

$$\frac{\mathrm{d}^2\mathrm{x(t)}}{\mathrm{dt}^2} = \mathrm{a(t)}$$

The best fit line should theoretically be perfectly horizontal, and its y-value should represent the average acceleration of the glider throughout the time interval. The data points seem to stray away from the actual acceleration more as time goes on. This is because the error is built up as the glider experiences more and more friction; it adds up and creates a bigger difference between the true acceleration and the measured acceleration. This is why the noise looks as it does.

If we take the average of all data points on the above plot, we should obtain an accurate value of the acceleration of the glider.

Applying Equation ii.11:[1]

$$\bar{a} = \frac{1}{N}\sum_{\mathrm{i}=1}^{N} a_{\mathrm{i}}$$

We have N = 59, so $\bar{a} = 19.92162$ cm/s². It should be noted that we assume $\bar{a} = a_{\mathrm{best}}$

To calculate the uncertainty corresponding to this acceleration value, we can use:

Applying Equation ii.13:[1]

$$\delta a = \frac{\sigma_a}{\sqrt{N}}$$

where σ_a is the standard deviation of the set of acceleration data

Excel calculates $\sigma_a = 37.76199$. $N = 59$, so we calculate $\delta a = 5$ cm/s². Therefore:

$$a = a_{\mathrm{best}} \pm \delta a$$

$$a = 20 \pm 5 \text{ cm/s}^2$$

This method for calculating acceleration is obviously much more inaccurate than the method in which we take the slope of the line of the velocity vs. time plot. The uncertainty in acceleration is significantly greater (uncertainty only to the ones digit) when we differentiate twice, proving the first method to be considerably more accurate (uncertainty to the tenths or even hundredths place). Despite the a_{best} values being nearly identical, the uncertainty difference is too great to ignore.

PRESENTATION MINI-REPORT

Exoplanets: From Detection to Detailed Characterization

The detection and study of exoplanets provides us with information about the universe that we are unable to observe within our own solar system. Once detected, a detailed analysis of the exoplanets reveals properties that are used to characterize each body. An accurate characterization and classification of exoplanets is necessary to ultimately determine which are habitable.[2] This review will mainly identify and describe methods for exoplanetary detection. It is also worth summarizing the properties of these planets that can be calculated from various detection methods, as well as presenting a more efficient way to discover exoplanets.

The emergence in discovery of exoplanets came with astrometry.[3] However, it was not until Doppler Velocimetry that successful detections became more frequent. The Doppler Technique proves the existence of exoplanets by detecting variation in a host star's radial velocity using spectroscopy and telescopes.[3] Radial Velocities (RVs) are analyzed and used to calculate fundamental properties, discussed later. One major limitation facing Doppler Velocimetry is the existence of stellar jitter.[3,4] Starspots induce stellar jitter, which may lead to unsuccessful or even false exoplanetary detection.[4] A possible solution posed to eliminate detection difficulties produced from stellar jitter is the technique known as Multi-Band Radial Velocity Exoplanet Detection, which takes into consideration the average temperature on the starspot and the spectral band amplitude ratio.[4] A correction equation developed by Bo Ma and Jian Ge[4] which takes into consideration the RV jitters has the form:

$$\mathrm{V_{exo,i}} = \frac{\alpha_\mathrm{i}\mathrm{V_{B,i}} - \mathrm{V_{A,i}}}{\alpha_\mathrm{i} - 1} \tag{1}$$

where A and B represent the different bands of spectra measured. $\mathrm{V_{A,i}} = \mathrm{V_{exo,i}} + \sigma_\mathrm{A,i}$, $\mathrm{V_{B,i}} = \mathrm{V_{exo,i}} + \sigma_\mathrm{B,i}$, and $\alpha_\mathrm{i} = \sigma_\mathrm{A,i}/\sigma_\mathrm{B,i}$ where starspot jitters are enveloped within $\sigma_\mathrm{A,i}$ and $\sigma_\mathrm{B,i}$.[4] As we can see, existing methods for detection are evolving in order to increase precision.

Another popular and effective technique for exoplanet detection is the Transit Method.[3,5,6] As bodies revolve around their host star, they may create an eclipse with respect to our line of sight from Earth to the star. Analysis of the eclipse shows a reduction in the star's brightness as the exoplanet passes through. Detection of brightness reduction therefore implies exoplanet existence around the host star.[5,6] The Transit method unfortunately encounters obvious limitations. Mainly, the exoplanet must orbit in the plane of our line of sight to its host star to produce any sort of brightness reduction.[5] Also, exoplanets too distant from their star or too small to produce brightness reduction will unlikely be detected.[5] Despite its limitations, this method is convenient in calculating exoplanetary properties in addition to Doppler Velocimetry.

Detecting exoplanets is only the first step in trying to study the universe beyond our solar system. To understand the nature of systems beyond ours, it is useful to determine the properties of exoplanets within that system and compare them to Earth and other planets within our solar system. Andrew Howard's review on the properties of exoplanets[6] provides a great analysis for how Doppler and Transit Methods can determine these properties. For example, the Doppler technique facilitates calculation of orbital periods, minimum mass, and eccentricity of orbit, all useful in determining habitability. The Transit Method, on the other hand, can measure a more unique property known as stellar obliquity: the angle between the host star's spin axis and its exoplanet's orbital axis.[6,7] When data is combined from Transit and Doppler evaluations, fundamental properties such as mass, radius, density, and orbital information can all be determined.[6]

The future of exoplanetary detection depends mostly on higher precision instrumentation.[3] However, one method that eliminates the limitations arising from the Doppler or Transit Method is known as Gravitational Microlensing.[8] This efficient technique allows for the detection of low-mass bodies located at relatively large distances from Earth. The basis behind gravitational microlensing is the deflection of a path of light. An image of a source of light travels through space and will be deflected by a lens created by a star located in between the source and the viewer (Earth). If the star has an orbiting exoplanet, the source image will be distorted, and we will observe a more complicated lens. This produces a phenomenon known as caustic lines.[8] Thus, using this method, we can detect even the smallest of the exoplanets at the furthest of distances from Earth.

Word Count: 694

References

[1] Campbell, W.C. et al. Physics 4AL: Mechanics Lab Manual (ver. April 3, 2017). (University of California Los Angeles, Los Angeles, California).

[2] Kasting, F. James, Whitmire, P. Daniel, Reynolds, T. Ray. Habitable Zones around Main Sequence Stars. *Icarus.* **101**, 108-128 (1993).

[3] Pepe, Francesco, Ehrenreich, David, Meyer, R. Michael. Instrumentation for the detection and characterization of exoplanets. *Nature.* **513**, 358-366 (2014).

[4] Ma, Bo, Ge, Jian. A New Multi-Band Radial Velocity Technique for Detecting Exoplanets around Active Stars. *The Astrophysical Journal.* **750**, 1-8 (2012).

[5] Bennett, O. Jeffrey. Life in the Universe. 362-365 (Pearson, 2017).

[6] Howard, W. Andrew. Observed Properties of Extrasolar Planets. *Science.* **340**, 572-576 (2013).

[7] Albrecht, Simon, Winn, N. Joshua. *et al.* Obliquities of Hot Jupiter Host Stars: Evidence for Tidal Interactions and Primordial Misalignments. *The Astrophysical Journal.* **757**, 1-25 (2012).

[8] Christie, W. G. Detecting Exoplanets by Gravitational Microlensing using a Small Telescope. *Society for Astronomical Science.* **1**, 1-8 (2006).